



HAL
open science

Convergent evolution of an extreme dietary specialisation, the olfactory system of worm-eating rodents

Quentin Martinez, Renaud Lebrun, Anang Achmadi, Jacob Esselstyn, Alistair Evans, Lawrence Heaney, Roberto Portela Miguez, Kevin Rowe, Pierre-Henri Fabre

► To cite this version:

Quentin Martinez, Renaud Lebrun, Anang Achmadi, Jacob Esselstyn, Alistair Evans, et al.. Convergent evolution of an extreme dietary specialisation, the olfactory system of worm-eating rodents. *Scientific Reports*, 2018, 8 (1), 10.1038/s41598-018-35827-0 . hal-02042569

HAL Id: hal-02042569

<https://hal.science/hal-02042569>

Submitted on 1 Feb 2021

HAL is a multi-disciplinary open access archive for the deposit and dissemination of scientific research documents, whether they are published or not. The documents may come from teaching and research institutions in France or abroad, or from public or private research centers.

L'archive ouverte pluridisciplinaire **HAL**, est destinée au dépôt et à la diffusion de documents scientifiques de niveau recherche, publiés ou non, émanant des établissements d'enseignement et de recherche français ou étrangers, des laboratoires publics ou privés.

SCIENTIFIC REPORTS



OPEN

Convergent evolution of an extreme dietary specialisation, the olfactory system of worm-eating rodents

Quentin Martinez¹, Renaud Lebrun¹, Anang S. Achmadi², Jacob A. Esselstyn^{3,4}, Alistair R. Evans^{5,6}, Lawrence R. Heaney⁷, Roberto Portela Miguez⁸, Kevin C. Rowe^{6,9} & Pierre-Henri Fabre¹

Turbinal bones are key components of the mammalian rostrum that contribute to three critical functions: (1) homeothermy, (2) water conservation and (3) olfaction. With over 700 extant species, murine rodents (Murinae) are the most species-rich mammalian subfamily, with most of that diversity residing in the Indo-Australian Archipelago. Their evolutionary history includes several cases of putative, but untested ecomorphological convergence, especially with traits related to diet. Among the most spectacular rodent ecomorphs are the vermivores which independently evolved in several island systems. We used 3D CT-scans (N = 87) of murine turbinal bones to quantify olfactory capacities as well as heat or water conservation adaptations. We obtained similar results from an existing 2D complexity method and two new 3D methodologies that quantify bone complexity. Using comparative phylogenetic methods, we identified a significant convergent signal in the rostral morphology within the highly specialised vermivores. Vermivorous species have significantly larger and more complex olfactory turbinals than do carnivores and omnivores. Increased olfactory capacities may be a major adaptive feature facilitating rats' capacity to prey on elusive earthworms. The narrow snout that characterises vermivores exhibits significantly reduced respiratory turbinals, which may reduce their heat and water conservation capacities.

Understanding how species have adapted to their environment is a major goal of evolutionary biology^{1–3}. Salient examples of convergence, the evolution of a similar trait in independent evolutionary lineages⁴, have demonstrated the importance of determinism through natural selection⁵. Recent advances in X-ray microtomography (X-ray μ CT) provide the opportunity to quantify convergence in morphological structures that are otherwise inaccessible^{5–7}. In mammals, the use of morphological proxies such as inner ears, braincase, floccular fossa, cribriform plate, and turbinal bones^{5–11} have shed light on ecological and functional adaptations, especially for taxa that are difficult to observe directly in the wild⁷.

Extensive studies of the mammalian olfactory subgenome revealed that mammals have a wide array of olfactory receptor genes that represent 1–6% of their genomes^{12–14}. The huge mammalian olfactory subgenome has proven useful to illustrate dietary and other adaptations^{12,15,16}. However, the nasal chamber of mammals has been relatively neglected by anatomists due to its internal position¹⁷, and few studies have tested for an adaptive link between nasal morphology and olfactory capacities^{18–20}.

¹Institut des Sciences de l'Evolution (ISEM, UMR 5554 CNRS-IRD-UM), Université de Montpellier, Place E. Bataillon - CC 064 - 34095, Montpellier Cedex 5, France. ²Museum Zoologicum Bogoriense, Research Center For Biology, Indonesian Institute of Sciences (LIPI), Jl. Raya Jakarta-Bogor Km.46, Cibinong, 16911, Indonesia. ³Museum of Natural Science, 119 Foster Hall, Louisiana State University, Baton Rouge, Louisiana, 70803, United States. ⁴Department of Biological Sciences, Louisiana State University, Baton Rouge, Louisiana, 70803, United States. ⁵School of Biological Sciences, 18 Innovation Walk, Monash University, Victoria, 3800, Australia. ⁶Sciences Department, Museums Victoria, Melbourne, Victoria, 3001 Australia. ⁷Field Museum of Natural History, 1400 S Lake Shore Drive, Chicago, 60605, United States. ⁸Natural History Museum of London, Department of Life Sciences, Mammal Section, London, United Kingdom. ⁹School of BioSciences, The University of Melbourne, Melbourne, Victoria, 3010, Australia. Correspondence and requests for materials should be addressed to Q.M. (email: quentinmartinezphoto@gmail.com)

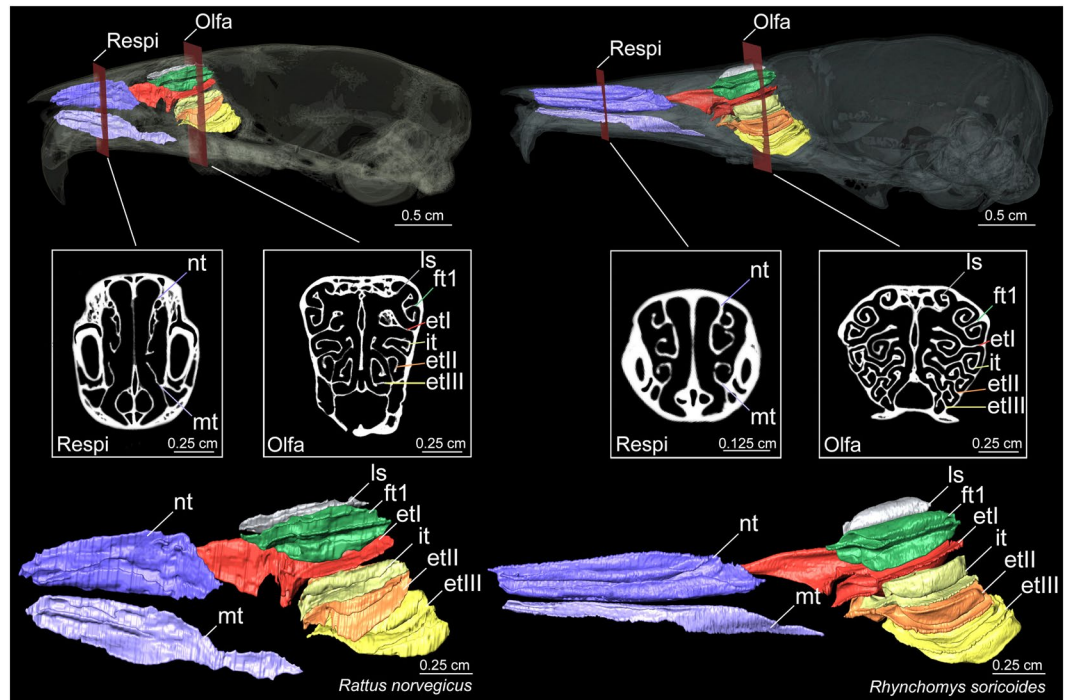


Figure 1. Coronal cross section and sagittal plane of skull and 3D representations of turbinal bones in *Rattus norvegicus* and *Rhynchomys soricoides*. Abbreviations: Respi = respiratory turbinals, Olfa = olfactory turbinals, nt = nasoturbinal, mt = maxilloturbinal, ls = lamina semicircularis, it = interturbinal, ft1 = frontoturbinal 1, etI = ethmoturbinal I, etII = ethmoturbinal II, and etIII = ethmoturbinal III.

In mammals, the nasal chambers contain bony plates called turbinals or turbinates, which are key structures involved in olfaction, thermoregulation, and water conservation. Because they bear the respiratory and olfactory epithelia^{8,9,17,21–24}, these turbinals have played a major role in the evolution of homeothermy and olfaction in mammals²⁵. Anatomists and physiologists usually distinguish two major functional parts for turbinals: (1) the respiratory and (2) the olfactory components (Fig. 1). The respiratory turbinals, which are anterior to the olfactory turbinals, are further divided into maxilloturbinals (MT) and nasoturbinals (NT, Fig. 1). Maxilloturbinals link the naris and nasopharynx and are covered by respiratory epithelium, a vascularised mucosa. During inhalation, they moisten and warm the breath; at exhalation, they conserve moisture^{17,23,26–29}. Nasoturbinals are located in the anterior portion of the nasal cavity, near the naris, and dorsal to the MT. They contribute to homeothermy, as suggested by their distal position from the olfactory bulbs, the presence of respiratory epithelium, airflow dynamics, and performance tests^{21,22,27,29–33}. However, NT probably also serve, at least partly, as olfactory structures³⁴ because they are partially covered by olfactory epithelium in groups such as rodents²⁴. As such, NT probably serve dual functions for olfaction and heat and water conservation^{21,22}. The olfactory turbinals are primarily associated with the olfactory process. They are covered by a thick olfactory epithelium, innervated by several olfactory receptors and directly connected to the close cerebral olfactory bulbs via olfactory nerves^{9,17,23,24,35–37}. In addition, olfactory turbinals are divided into several structures variably named lamina semicircularis (ls), frontoturbinals (ft), interturbinals (it), and ethmoturbinals (et, Fig. 1)^{38–41}.

Studies of carnivorans suggest a possible link between olfactory turbinal size and olfactory performance as well as between respiratory turbinal size and heat or moisture conservation performance^{8,9,42}. The physiological importance of turbinal bones was thereby shown by the correlation between surface areas of these bones and species' ecological traits. These studies have especially demonstrated the correlation between dietary adaptations and the surface area of olfactory turbinals²³. However, these types of studies are rare outside of carnivorans, leaving open the question of whether connections between ecological traits and turbinal surface areas is a general pattern.

Rodents of the family Muridae have migrated from mainland Asia to the many islands of the Indo-Australian Archipelago (IAA) multiple times since the Miocene^{43,44}. These small to medium-sized mammals have spread over most of the IAA, where they occupy many terrestrial niches^{43,44}. Included among this diversity are the “shrew-rats”, carnivorous rodents (i.e., those that feed on metazoans) that evolved independently in New Guinea, the Philippines, and Sulawesi^{44–47}. Shrew-rats are an ideal comparative system to study dietary specialisation because they have convergently evolved from an ancestral omnivorous diet toward carnivory⁴⁴. This adaptation appeared at least five times in the highly diverse Murinae, with at least two origins of highly specialised carnivorous lineages: (1) the Sulawesi shrew-rats and (2) the Philippine shrew-rats. Several species of shrew-rats consume a wide-range of invertebrates, but others are earthworm specialists with spectacular changes to their rostrum morphology. In the most specialised vermivorous species (*Paucidentomys* and *Rhynchomys* genera), the snout is extremely long and narrow^{44,45,48} and might have constrained the size and shape of turbinals. Additionally,

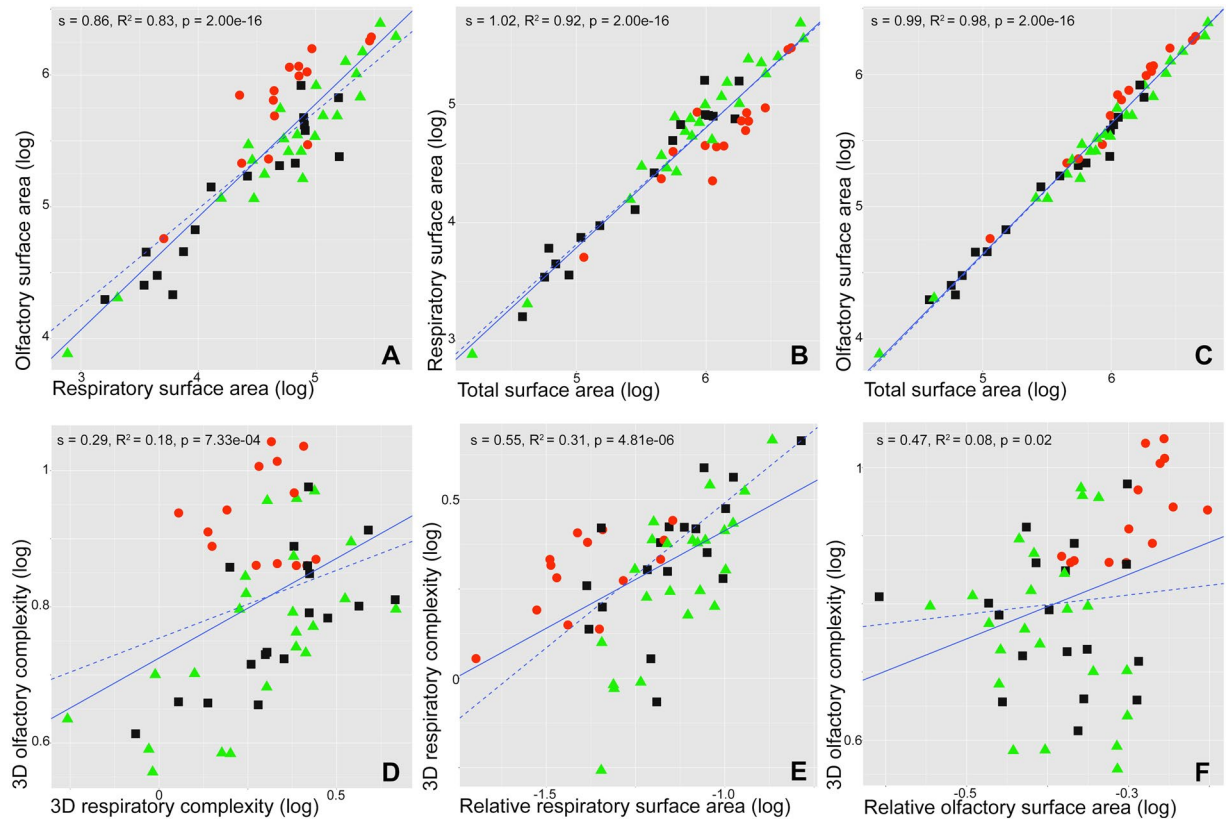


Figure 2. Log–log regressions (continuous line) and PGLS (dashed line) of (A) olfactory vs respiratory turbinal surface area, (B) respiratory vs total surface area, (C) olfactory vs total surface area, (D) olfactory vs respiratory 3D complexity (CHAR), (E) respiratory 3D complexity (CHAR) vs relative respiratory surface area, and (F) olfactory 3D complexity (CHAR) vs relative olfactory surface area. Colours and symbols: red dots = vermivorous, black squares = carnivorous, and green triangles = omnivorous.

the snout morphology of these vermivores might involve increased olfactory capacities to detect earthworms in leaf-litter.

Using comparative phylogenetic methods, we contrasted turbinal surface area and turbinal complexity between vermivorous, carnivorous and omnivorous species of Murinae to test hypothesised adaptations related to olfaction and heat and moisture conservation in the shrew-rats. We tested for convergence of the vermivorous pattern. In doing so, we propose two new indices of three dimensional (3D) complexity of turbinal bones, which we have implemented in the freeware MorphoDig⁴⁹.

Results

Turbinal surface area. There is a significant correlation between surface area of all turbinals and skull length (electronic supplementary material (ESM), Fig. S3A; slope (s) = 2.25, r squared (R^2) = 0.88, p -value (p) = 2.00e-16). The surface area of all turbinals show strong positive allometry (s = 2.25). The PGLS slope of vermivores is significantly different from the PGLS slope of carnivores and omnivores (p = 0.01 and 0.02, respectively; ESM, Fig. S3A). This indicates that when skull length increases, vermivores have a smaller increase in turbinal surface area than do carnivores and omnivores. This surface area difference could be explained by the smaller area of the respiratory turbinals (ESM, Fig. S3B). In fact, the PGLS slope of respiratory turbinal area and skull length in vermivores is significantly different from that of carnivores and omnivores (p = 0.01 in both cases; ESM, Fig. S3B). Furthermore, there are no PGLS slope differences between dietary categories for the correlation between olfactory turbinal surface area and skull length (p > 0.05; ESM, Fig. S3C). There is a significant correlation between olfactory and respiratory surface area (Fig. 2A; slope (s) = 0.86, R^2 = 0.83, p = 2.00e-16) and these variables display a negative allometry (s = 0.86). There are significant correlations between the surface area of respiratory or olfactory turbinals and the surface area of all turbinals (Fig. 2B and C; s = 1.02, R^2 = 0.92, p = 2.00e-16 and s = 0.99, R^2 = 0.98, p = 2.00e-16, respectively). PGLS slopes do not differ significantly between dietary categories for these two correlations (p > 0.3; Fig. 2B, C) and the relationship between these variables is isometric (s = 1.02 and s = 0.99; Fig. 2B, C). This suggests that sampled species exhibit the same relationship for these variables, thereby allowing comparisons of respiratory and olfactory turbinals between dietary categories.

ANOVA reveals that the residuals of PGLS (resPGLS) between olfactory and respiratory turbinals surface area is significantly affected by diet (p = 2.62e-07; ESM, Table S2). Indeed, vermivores have resPGLS between the

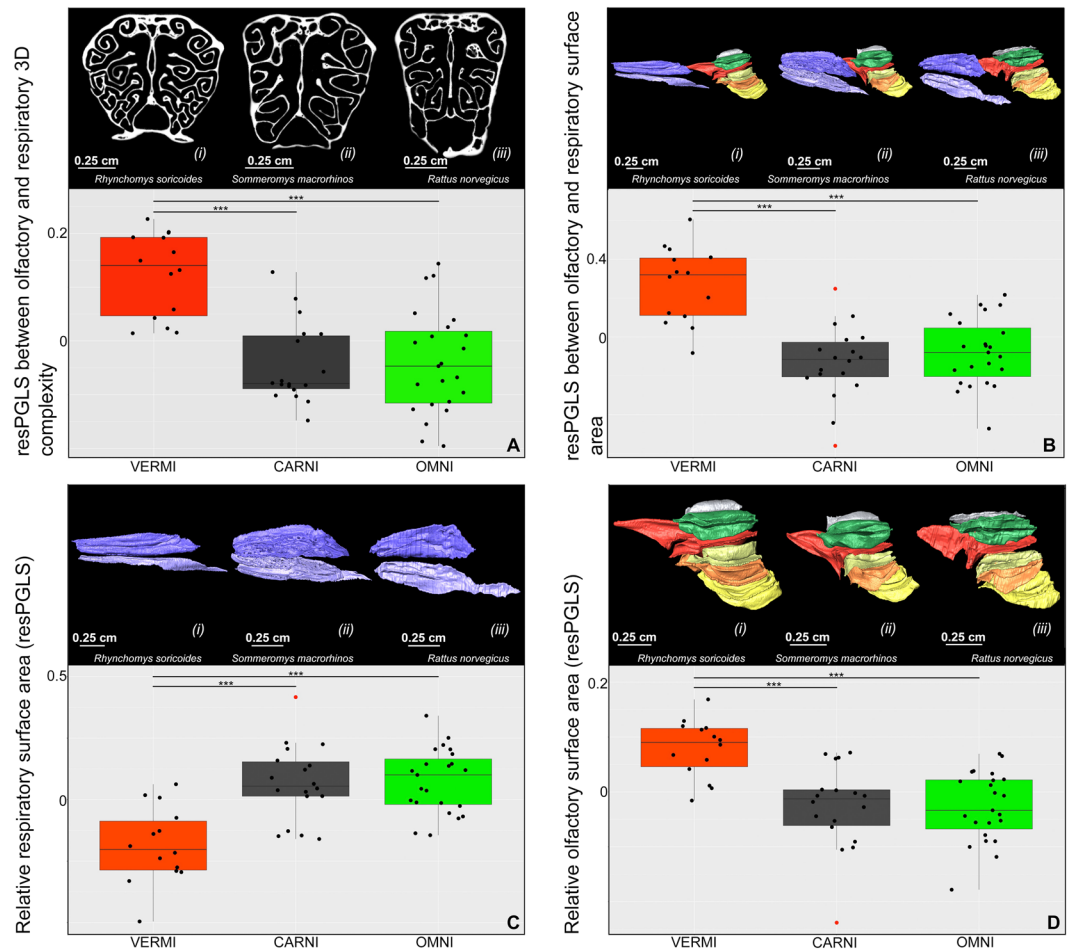


Figure 3. Boxplot with dietary categories: (A) residuals of PGLS (resPGLS) between olfactory and respiratory 3D complexity of turbinals (CHAR), (B) resPGLS between olfactory and respiratory surface area, (C) relative respiratory surface area (resPGLS), and (D) relative olfactory surface area (resPGLS). Significance codes are based on phylogenetic Tukey's HSD test. (i) *Rhynchomys soricoides*, (ii) *Sommeromys macrorhinos*, and (iii) *Rattus norvegicus*. Colours: red = vermivorous, black = carnivorous, and green = omnivorous. Red points are outliers.

surface area of olfactory and respiratory turbinals significantly higher than carnivores and omnivores (Fig. 3B; $p = 1.00 \times 10^{-4}$; ESM, Table S3). Phylogenetic ANCOVA shows similar results with significant differences between vermivorous and carnivorous dietary categories ($p = 1.43 \times 10^{-8}$; ESM, Table S6). Considering the nasoturbinale either as olfactory or as respiratory turbinals does not significantly change the results (ESM, Table S4). Moreover, slope differences between linear regressions and PGLS are small (ESM, Table S1). Differences between phylogenetic and non-phylogenetic Tukey's HSD tests are also small (ESM, Table S5).

ANOVA reveals that the relative surface area of olfactory turbinals is significantly affected by diet ($p = 2.62 \times 10^{-7}$; ESM, Table S2). Indeed, vermivores have significantly higher relative surface area of olfactory turbinals as compared to carnivores and omnivores (Fig. 3D; $p = 9.17 \times 10^{-5}$ and 8.40×10^{-5} , respectively; ESM, Table S3). Phylogenetic ANCOVA shows similar results with significant differences between vermivorous and carnivorous dietary categories ($p = 8.46 \times 10^{-7}$; ESM, Table S6).

ANOVA reveals that the relative surface area of respiratory turbinals is significantly affected by diet ($p = 4.11 \times 10^{-6}$; ESM, Table S2). Indeed, vermivores have significantly smaller relative respiratory turbinal surface area, relative nasoturbinale surface area, and relative maxilloturbinal surface area than do carnivores and omnivores (Fig. 3C; $p = 1.18 \times 10^{-5}$, 1.00×10^{-5} , 2.67×10^{-4} , 2.19×10^{-4} , 4.47×10^{-3} , and 1.34×10^{-3} , respectively; ESM, Fig. S4A, B, Table S3). Phylogenetic ANCOVA shows similar results with significant differences between vermivorous and carnivorous dietary categories ($p = 8.46 \times 10^{-7}$; ESM, Table S6).

Turbinal complexity. Olfactory and respiratory 3D complexity are significantly correlated (CHAR, Fig. 2D; $s = 0.29$, $R^2 = 0.18$, $p = 7.33 \times 10^{-4}$). Olfactory 3D complexity (CHAR) and skull length are also significantly correlated (ESM, Fig. S3E; $s = 0.27$, $R^2 = 0.27$, $p = 2.60 \times 10^{-5}$). ANOVA reveals that resPGLS between olfactory and respiratory 3D complexity (CHAR) is significantly affected by diet ($p = 3.59 \times 10^{-7}$; ESM, Table S2). Indeed, vermivores have a significantly higher resPGLS between the 3D complexity (CHAR) of olfactory and respiratory turbinals compared to carnivores and omnivores (Fig. 3A; $p = 2.70 \times 10^{-6}$ and 1.60×10^{-6} , respectively). Phylogenetic

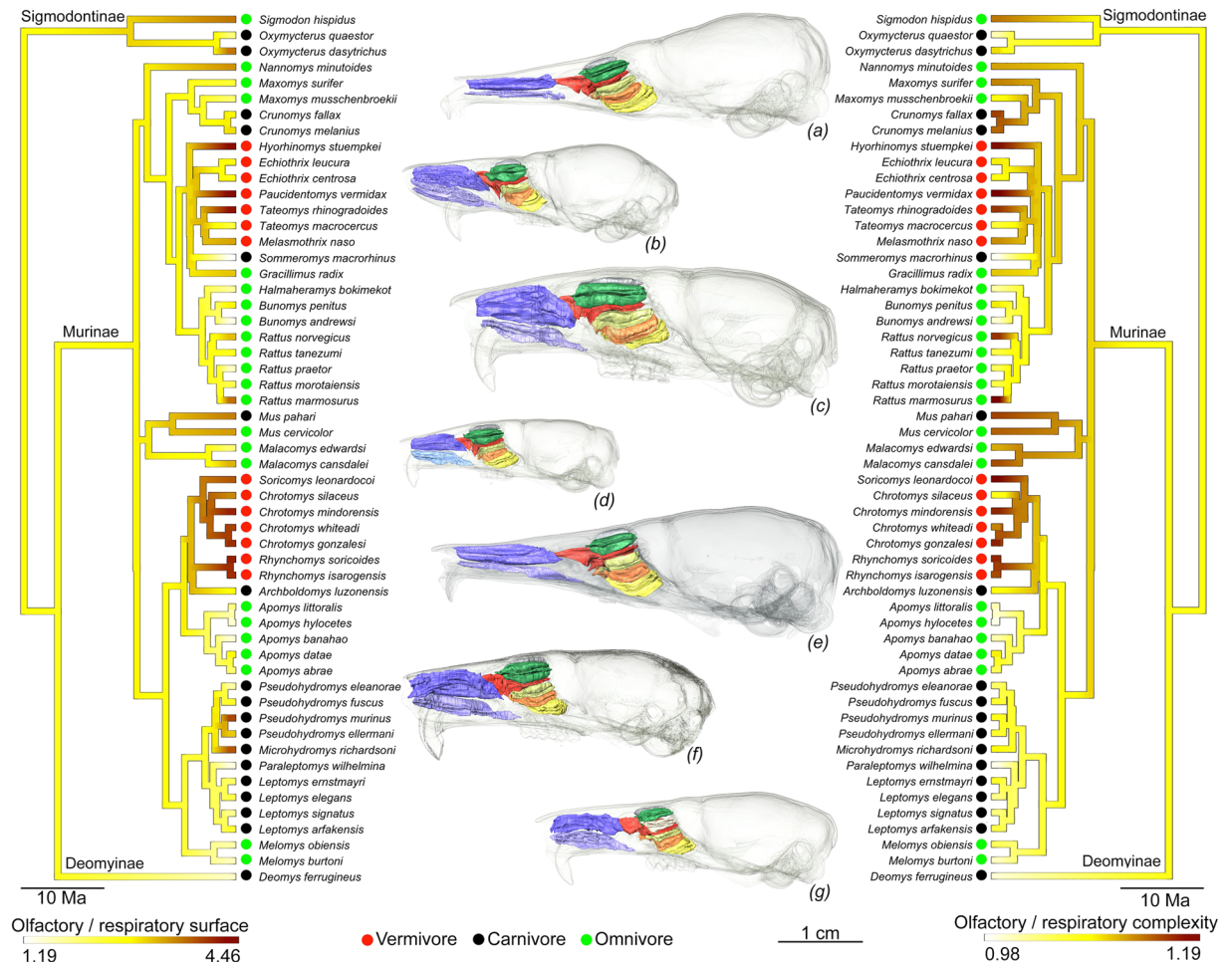


Figure 4. Continuous mapping of the ratio between olfactory and respiratory turbinal surface area (left) and of the ratio between olfactory and respiratory turbinal 3D complexity (CHAR, right) with phylogenetic relationships. (a) *Paucidentomys vermidax*, (b) *Sommeromys macrorhinos*, (c) *Bunomys penitus*, (d) *Mus pahari*, (e) *Rhynchomys soricoides*, (f) *Apomys banahao*, and (g) *Deomys ferrugineus*.

ANCOVA shows similar results with significant differences between vermivorous and carnivorous dietary categories ($p = 1.82e-03$, ESM, Table S6). Slope differences between linear regressions and PGLS are low (ESM, Table S1). 3D complexity (CHAR) of olfactory turbinals is significantly affected by diet ($p = 8.54e-05$). Indeed, vermivores and carnivores express a significantly higher olfactory turbinal complexity than omnivores ($p = 5.42e-05$ and $p = 0.05$, respectively; ESM, Table S3). Respiratory turbinals 3D complexity (CHAR) is not significantly affected by diet ($p = 0.14$; ESM, Table S2).

Results obtained with our two 3D complexity indices are similar to each other (ESM, Fig. S5 and Table S3) and to those obtained from 2D complexity (ESM, Fig. S5 and Table S3). This indicates that the 2D complexity signal from the middle slice of each turbinal group extracts the complexity of each turbinal group.

Turbinal surface area and turbinal complexity. There is a significant correlation between 3D complexity (CHAR) and relative surface area of respiratory turbinals (Fig. 2E; $s = 0.55$, $R^2 = 0.31$, $p = 4.81e-06$). Considering phylogeny, there is no significant correlation between the 3D complexity (CHAR) and the relative surface area of olfactory turbinals (Fig. 2F; PGLS $s = 0.14$, PGLS $p = 0.36$). The continuous phylogenetic mapping of the ratio between olfactory and respiratory surface areas and 3D complexity (CHAR) reveals similar patterns for both proxies (surface area and complexity; Fig. 4). However, four species display a different pattern between these two proxies: *Chrotomys silaceus*, *Maxomys surifer*, *Microhydromys richardsoni*, and *Pseudohydromys murinus* (Fig. 4). Even if patterns between surface area and 3D complexity (CHAR) are similar (Fig. 4), very low R^2 values in some PGLS (Fig. 2; ESM, Fig. S3, and Table S1) reveal that we need to consider both proxies to understand olfactory capacities.

Snout. Snout length and width differences are significantly affected by diet when vermivores are separated into two ecological subcategories: terrestrial and semi-fossorial vermivores ($p = 0.01$, $p = 1.09e-04$, respectively; ESM, Table S2). Indeed, semi-fossorial vermivores (*Chrotomys* spp.) have significantly shorter snouts than carnivores and terrestrial vermivores ($p = 0.04$, $p = 0.03$, respectively; ESM, Table S3). Terrestrial vermivores have

Model	(A) RespiSA/TotSA		(B) OlfaSA/TotSA		(C) OlfaSA/RespiSA		(D) OlfaCHAR		(E) OlfaCHAR/RespiCHAR	
	AICc	ΔAICc	AICc	ΔAICc	AICc	ΔAICc	AICc	ΔAICc	AICc	ΔAICc
BM	-132.63	34.35	-132.63	34.35	453.76	1127.27	-94.73	15.01	-127.42	62.83
OU1	-161.79	5.20	-161.79	5.29	-668.09	5.42	-107.18	2.56	-186.47	3.78
OU2	-166.99	0.00	-166.98	0.00	-673.51	0.00	-109.74	0.00	-190.25	0.00
OU3	-164.58	2.40	-164.59	2.40	-669.04	4.47	-107.50	2.25	-185.76	4.49

Table 1. Results of 1 000 simulations of single-rate BM and three alternative OU models with (A) the ratio between respiratory and total surface area, (B) the ratio between olfactory and total surface area, (C) the ratio between olfactory and respiratory surface area, (D) the 3D olfactory complexity (CHAR), and (E) the ratio between olfactory and respiratory 3D complexity (CHAR). BM and OU1 with omnivorous and all carnivorous dietary categories (carnivorous + vermivorous); OU2 with omnivorous, carnivorous, and vermivorous dietary categories; and OU3 with omnivorous, carnivorous, terrestrial vermivorous, and semi-fossorial vermivorous dietary categories. AICc = Akaike's information criterion corrected. ΔAICc = difference between AICc compared to minimum AICc.

Variables	C1	p-value	C2	p-value	C3	p-value
RelatOlfaSA + RelatRespiSA + OlfaCHAR + SNW	0.233	0.123	0.11	0.002	0.122	0.113
RelatOlfaSA + RelatRespiSA + OlfaCHAR	0.394	0.003	0.163	<1.000e-04	0.207	0.005
RelatOlfaSA + OlfaCHAR	0.408	0.009	0.165	<1.000e-04	0.217	0.003

Table 2. Results of the three convergence index tests as proposed by Stayton 2015¹⁰⁶ with: RelatOlfaSA = relative olfactory surface area, RelatRespiSA = relative respiratory surface area, OlfaCHAR = olfactory 3D complexity of the convex hull area ratio, and SNW = snout width.

significantly narrower snouts than omnivores and semi-fossorial vermivores (ESM, Fig. S6; $p = 0.02$ and $6.03e-05$, respectively; ESM, Table S3). Semi-fossorial vermivores (*Chrotomys* spp.) have significantly larger relative snouts compared to omnivores, carnivores, and terrestrial vermivores (ESM, Fig. S6; $p = 0.01$, $2.00e-03$, and $6.03e-05$, respectively; ESM, Table S3).

Adaptation and convergence. The best-fitting model is OU2 (Table 1), a model with 3 adaptive optima: omnivorous, carnivorous, and vermivorous dietary categories for (A) relative respiratory surface area, (B) relative olfactory surface area, (C) olfactory and respiratory surface area, (D) 3D complexity (CHAR) of olfactory turbinals, and (E) 3D complexity (CHAR) of olfactory and respiratory turbinals. The best fitting model for the relative snout width is OU3 (ESM, Table S7), with 4 adaptive optima: omnivorous, carnivorous, terrestrial vermivorous, and semi-fossorial vermivorous diets and lifestyles.

Considering the C2 index, vermivorous murine convergence is highly significant when we test for global rostral pattern composed of relative olfactory and respiratory surface area, olfactory 3D complexity (CHAR), and snout width (Table 2). The convergence is not significant when we consider the C1 and C3 indices (Table 2). Considering the three indices (C1, C2, and C3), the convergence is highly significant when we test for the relative olfactory surface area, the respiratory surface area, and the olfactory 3D complexity (Table 2); or when we test for the relative olfactory surface area and the olfactory 3D complexity (Table 2).

Discussion

Olfactory capacities in vermivorous murines. Compared to carnivores and omnivores, vermivores should have significantly better olfactory capacities, based on both the larger surface area and higher complexity of their olfactory turbinals. We hypothesised that these bony specialisations are related to an improvement of their olfactory adaptations allowing them to detect prey that are underground or invisible within wet leaf litter (Heaney, pers. comm). Such prey may be especially elusive and difficult to detect for more generalist, opportunistic rats. Indeed, molecular odorants are especially difficult to detect underground as compared to on the surface⁵⁰. Most of these insular vermivorous rats (*Melasmothrix*, *Soricomys*, and *Tateomys*) are terrestrial and display relatively long claws in order to dig into moss, bark, leaf litter, and damp soil, where these earthworms are most abundant⁵¹. Other earthworm specialists patrol runways (*Echiothrix* and *Rhynchomys*)^{45,52} or dig underground (*Chrotomys*)⁵² to find their prey. The wide and short snout of the semi-fossorial vermivorous *Chrotomys* (ESM, Table S3 and Fig. S6) might be a fossorial adaptation that is also found in other fossorial rodents like chisel-tooth diggers^{53,54}. Following Heth & Todrank⁵⁰, the semi-fossorial vermivorous *Chrotomys* should have higher olfactory capacities than terrestrial ones, in order to detect molecular odorants from their underground prey. Based on turbinal complexity and surface area measurements some vermivores display the most derived morphology relative to the sampled murines with the highest olfactory capacities. This occurs with semi-fossorial species (*Chrotomys* spp.), with species that are patrolling along runways (*Rhynchomys isarogensis* and *R. soricoides*), that dig into bark (*Tateomys rhinogradoides*) and some with unknown feeding behaviours (*Hyorhinomys stuempkei* and *Paucidentomys vermidax*; Figs. 3 and 4). As our results show, the morphological diversity of these vermivores is quite large and we have a rather limited knowledge about their ecological diversity. Ecological studies of rodents are difficult due to most species' nocturnal activity, poor trapping success, and sometimes low abundance, especially in the case of the vermivores⁵⁵⁻⁵⁷. It will be important in the future to investigate in greater detail stomach

contents using metabarcoding if we are to understand the link between olfactory capacities and dietary behaviors of vermivorous rats. Different ecomorphs of earthworm specialists might occur in different underground and ground layers. Our results reveal a connection between dietary specialisations and surface area and complexity of olfactory turbinals, which suggests a functional link. However, these lines of morphological evidence are just a first step toward understanding the ecological and functional diversity of shrew-rats. While the link between the size of olfactory organs or the number of olfactory receptors and olfactory performance is debated^{9,18–20,58,59}, mammals show a strong correlation between the size of a morphological proxy for olfaction (the cribriform plate) and the repertoire of olfactory receptor genes (OR)¹¹.

To our knowledge, there is no study showing a clear relation between olfactory performances and the size of olfactory proxies such as turbinal bones, cribriform plate, olfactory bulb or vomeronasal organ. This lack of knowledge does not allow us to discriminate between acuity, sensitivity, and discrimination when we used olfactory turbinal proxies. However, our findings about the highly specialised vermivores suggest that an increasing in olfactory turbinal size is probably not correlated with odorant acuity, that is the ability to detect a wide array of odorants⁹. Integrative studies of the olfactory system that include performance tests will further our understanding of these distinctive animals.

Heat and moisture conservation. In terrestrial vermivores, the distal part of the snout is narrow (ESM, Table S3 and Fig. S6), which is assumed to be a morphological adaptation to earthworm consumption^{60–62}. Such snout morphology has profound consequences for the respiratory surface and complexity of turbinals. Under a trade-off hypothesis between olfactory and respiratory turbinals, respiratory turbinal reduction could be a consequence of the increased size of olfactory turbinals. Indeed, previous work on carnivores⁹ suggests a trade-off between olfactory and respiratory turbinal areas due to the limited rostral space and the need for other functions, such as vision or cranio-mandibular muscles. Additionally, the highly specialised cranio-mandibular apparatus of vermivores⁴⁸ might impact the evolution of their rostrum, and the narrowing trend has resulted in highly reduced surface of the naso- and maxilloturbinal bones (Fig. 3C and ESM, Table S3 and Fig. S4). Depending on the organism and their environmental conditions, the respiratory turbinals may be involved in water conservation (e.g., in salty or dry environments) or heat retention (e.g., in cool or aquatic environments)^{8,17,26–32,63}. Despite wide altitudinal and thermal differences in the sampled murines, the reduction of heat and moisture conservation potential in vermivores may not present a major energetic constraint in their tropical and terrestrial environments. Under the trade-off hypothesis between respiratory and olfactory turbinals, respiratory turbinal reduction might have facilitated an increase of olfactory capacities as the novel cranio-mandibular specialisations developed in vermivorous lineages.

Vermivores convergence. Claims of convergence were previously proposed for vermivorous murines based on discrete character observations^{44,51}, or by the use of a common vernacular name: shrew-rats. Dietary convergences in both insular and continental murids were recently demonstrated with stomach content evidence⁴⁴. Using a large-scale phylogenetical framework for murids, Rowe⁴⁴ inferred ancestral dietary state and recorded at least 7 shifts from an omnivorous to a carnivorous diet, with a potential reversal from carnivory to omnivory in *Gracilimus*⁶⁴. Our results demonstrate a strong convergence footprint involving aspects of both the rostrum and turbinal morphologies (Tables 1, 2, and ESM, Table S7). Specifically, convergence among shrew-rats involves larger and more complex olfactory turbinals (Fig. 3A, B, D, 4, and ESM, Table S3), reduced respiratory turbinals (Fig. 3C and ESM, Table S3 and Fig. S4), and narrower snouts (ESM, Table S3 and Fig. S6). As explained in previous sections, these convergent patterns are probably related to dietary adaptations within the most specialised vermivorous forms.

Convergence among these shrew-rats might have been fostered by their replicated colonisation of islands in the Indo-Australian Archipelago, a hypothesis that is in accordance with the insular adaptive radiation theory^{65,66}. However, colonisation of islands is not the only factor that might have led to the convergence of these lineages that are mainly found on the largest islands with mountainous landscapes^{52,64}. Indeed, most IAA vermivores occur at relatively high elevation^{47,52,67–69}. This distribution pattern coincides with an increase in earthworm density and abundance, demonstrated along elevation transects both in Luzon (Philippines) and Borneo (Malaysia)^{55,70}. Rowe *et al.*⁴⁴ suggested that the altitudinal distribution of vermivores might be explained by increased earthworm abundance as well as the reduction of potential food competitors such as ants that are most abundant in the lowlands^{55,71,72}. Richness and abundance of small mammals is also higher at high altitude in islands of the IAA^{57,72–75}. Inter-specific interaction of small mammals is another hypothesis to explain the diversity of these vermivores, especially on islands. Both high species richness and high competition for resources in these small mammal communities might have fostered these convergences. In fact, their omnivorous ancestors independently took advantage of an ecological niche that was likely vacant, mainly in an insular context. Specialisation into shrew-rat ecomorphs (runner, digger, and fossorial) might have reduced food competition and allowed co-occurrence of several earthworm specialists that likely share diverse earthworm resources at mid- to high elevations on islands. The successful dietary specialisation of vermivores was associated with independent acquisitions of large and complex olfactory turbinal bones that presumably improved olfactory capacities. Beyond the morphological convergence of molar reduction⁶² and turbinal bones, other convergent aspects will certainly be revealed by future anatomical and functional studies.

Conclusion

Despite recent studies about mammal olfaction^{11,16,76,77} our knowledge in this field is rather limited. For example, the olfactory and respiratory epithelial covers are unknown or poorly described in most of non-model species. Comparative histology will help to refine the functional discrimination between olfactory and respiratory turbinals. Additionally, very few studies have been done concerning the complexity of turbinal bones^{8,9,28,77,78}.

Consequently, further studies will be necessary to understand the functional role of the complexity in nasal air-flow and odorant deposition⁷⁹. Despite this first evidence showing the possible trade-off between respiratory and olfactory turbinal bones (Fig. S3) further studies should use other variables than the skull length to test this hypothesis. Indeed, skull length might covary with nasal cavity and turbinal bones. Finally, other anatomical proxies should be further investigated such as the nasal septum, the cribriform plate, the olfactory bulb or the vomeronasal organ to understand multiple factors of murine olfaction.

Turbinal bones are important structures to understand how species that are challenging to study in the field have adapted to their environment. Consequently, museum specimens with undamaged turbinates are very valuable. Over the past few years there is an emerging trend to request samples of turbinal bones from museum specimens for molecular work (R. Portela Miguez in pers.). In light of the findings of our research, we recommend that the integrity of these nasal structures should be preserved so others can replicate this study or investigate other species applying similar methods.

Material and Methods

We borrowed 87 skulls belonging to 55 rodent species from: American Museum of Natural History (AMNH), Centre de Biologie et de Gestion des Populations (CBGP), Field Museum of Natural History (FMNH), Museums Victoria (NMV), Museum Zoologicum Bogoriense (MZB), Natural History Museum London (NHMUK), Natural History Museum of Paris (MNHN), Smithsonian Institution National Museum of Natural History (NMNH), and University of Montpellier (UM). These samples comprised 14 vermivorous (30 specimens), 18 carnivorous (28 specimens), and 23 omnivorous species (29 specimens (ESM, Tables S8 and S9)). All sampled species were considered terrestrial except for *Chrotomys*, a semi-fossorial genus^{52,55,56}. For outgroups, we selected additional carnivorous and omnivorous genera in Cricetidae (*Oxymycterus* and *Sigmodon*) and Muridae (Deomyiinae).

Digitising and measurement. Skulls were scanned using X-ray microtomography on a SkyScan 1076 (ISEM Institute, Montpellier), Nikon Metrology HMX ST 225 (NHMUK Natural History Museum, London), or SkyScan 1174v2 (The Evans Evolutionary Morphology Lab, Monash University, Melbourne). Acquired voxel size ranged from 18 to 36 μm . We digitised each left turbinal from each individual with Avizo Lite 9.0.1 software (VSG Inc., Burlington, MA, USA). This process was completed by semi-automatically selecting and delimiting each turbinal on each reconstructed virtual slice. Segmentation followed turbinal descriptions presented for Rodentia⁸⁰, Lagomorpha³⁸, and Marsupialia⁸¹. According to these references, we divided into 8 or 9 turbinals (Fig. 1 and ESM, Figs. S1 and S2) and followed anatomical terminology of ontogeny^{38–41}. For the lamina semicircularis, we segmented only the homologous branching part (Fig. 1 and ESM, Figs. S1 and S2) that is covered by olfactory epithelium²⁴. We identified an additional frontoturbinal (ft2) positioned between ft1 and et1 (ESM, Fig. S2), which is only present in the outgroups (Deomyiinae and Sigmodontinae). A second interturbinal (it) was also found in one individual of *Tateomys macrocercus* (Murinae). These additional turbinals were used in quantitative analyses of olfactory surfaces because they are located in the olfactory recess and should be covered by epithelial olfactory cells as are other olfactory turbinals²⁴. Following previous comparative studies works that used turbinal bone surface area^{9,23}, we decide to not include other bone structures that are covered by epithelium other than turbinals. For example, the nasal septum is partially covered in sensory epithelium^{17,24,82} but accurate delimitation is not possible with dry skulls. For all following quantitative measures and analyses, we took species averages for which we have multiple specimens (ESM, Table S8).

Skull length (SKL) was measured between the most anterior part of the nasal bone and the most posterior part of the occipital bone⁸³. Snout length (SNL) was measured between the most anterior part of the nasal bone and the posterior-most portion of the naso-frontal suture. The snout width (SNW) was measured across the nasolacrimal capsules⁸³. Length measurements were exported using Avizo Lite 9.0.1 software (VSG Inc., Burlington, MA, USA).

Turbinal surface area. We divided the turbinals into olfactory and respiratory regions to estimate the surface area available for these two functions and used the surface area as a proxy for olfactory or heat and moisture conservation capacities. Due to the impossibility of estimating the proportion of nasoturbinal that was involved in olfaction or in heat and moisture conservation, we performed separate surface area analyses including nasoturbinal either as respiratory or as olfactory turbinals (ESM, Table S4). Within turbinal regions, we assumed that the different epithelial cells and receptors were evenly distributed and as such, greater surface area indicates greater capacity. We sized turbinal surface areas by the total surface area of all turbinals. The surface area of segmented turbinals were exported using Avizo Lite 9.0.1 software (VSG Inc., Burlington, MA, USA).

Turbinal complexity. In addition to surface area, we also used turbinal complexity as a proxy for olfactory and heat or moisture conservation capacities. We interpret complexity as the degree of details in a predefined area. Following the principles of fluid dynamics, proportionally more fluid volume will come in contact with the edge of a narrow pipe than in a larger pipe. We assume that the same rule applies to air as it passes by the turbinals. As such, turbinals should be more efficient for surface exchange in complex structures than in simpler ones. As an example, a species with a high olfactory turbinal complexity is hypothesised to have good olfactory capacities.

To measure 2D turbinal complexity, we used the box counting method^{84,85}. The complexity value (Db) was based on the number of boxes placed into a grid and necessary to cover the shape border, changing box size from large to small. It is a ratio between the details and the total scale, quantifying the fractal dimension of the bone. To simplify the process of 2D complexity acquisition, we measured turbinal complexity for each respiratory and olfactory turbinal group. We considered that all anteriorly positioned turbinals (respiratory turbinals) were involved in heat and moisture conservation, while posterior ones (olfactory turbinals) participated in

olfaction. Using ImageJ software⁸⁶, we extracted scanned images corresponding to the middle of the total number of slices composing each turbinal group. We converted the turbinal shape into a single pixel-wide binary contour using skeletonisation. The image was then scaled and centered onto a 300 × 300-pixel black square with Adobe Photoshop CS6 software. Images were converted to grayscale and binary formats. The 2D complexity value was obtained with ImageJ plugin FracLac⁸⁷. Slice surface area was used as a size proxy to scale complexity values.

To measure 3D turbinal complexity we propose two indices implemented in the freeware MorphoDig⁴⁹. These indices both make use of 3D convex hulls. A convex hull is the smallest convex envelope that contains the studied shape, in our case the turbinal bones.

Firstly, the convex hull area ratio (CHAR) is the ratio between the turbinal surface area (SA) and the surface area of the corresponding convex hull (CHSA):

$$CHAR = \frac{SA}{CHSA}$$

Secondly, the convex hull normalised shape index (CHNSI) measures how much turbinal surface area (SA) can be enclosed within the volume defined by the convex hull of the turbinal (CHV). It is defined as:

$$CHNSI = F \frac{\sqrt[3]{SA}}{\sqrt[3]{CHV}}$$

where F is a constant defined so that spherical shapes express a CHNSI index equal to 1, as the 3D convex hull of a given:

$$F = \frac{\sqrt[3]{\frac{4}{3}\pi}}{2\sqrt{\pi}}$$

Quantitative analyses. We performed phylogenetic generalized least squares (PGLS) using R v.3.2.4⁸⁸, with ape⁸⁹, nlme⁹⁰, and phytools⁹¹. The phylogeny used for the following analyses was adapted from Fabre *et al.*, Rowe *et al.*, and Steppan & Schenk (^{43,44,92}, ESM, legend S1). To determine if slopes were significantly different between dietary groups and to compare allometric effects, we performed analysis of covariance (ANCOVA) following Claude⁹³. We also performed analysis of variance (ANOVA) based on the residuals of PGLS (resPGLS) to test for dietary influence on turbinal surface area, turbinal complexity, snout length, and snout width. To test for group differences, we performed the multiple comparison test of Tukey's HSD based on the residuals of the PGLS with the R package multcomp⁹⁴. To compare differences without phylogeny we also performed Tukey's HSD tests based on the residuals of linear regressions. For all analyses based on PGLS we performed model fitting with: a model without phylogeny, Brownian (BM), Ornstein–Uhlenbeck (OU), and Grafen models in order to adapt the phylogenetic model to our data^{95,96}.

Because methodological studies pointed out some biased results when residuals are treated as data^{97–99}, we compared our residual approach with phylogenetic ANCOVA (ESM, Table S6). We contrasted three models: a model without dietary categories (H0), a model with omnivorous and carnivorous dietary categories (Carni), and a model with omnivorous, carnivorous, and vermivorous dietary categories (Vermi). Models were compared using the Akaike information criterion (AIC) and the Likelihood-ratio test (LRT).

Adaptation and convergence tests. To test for associations between dietary categories and turbinal surface area, turbinal complexity, snout length, and snout width, we fit Brownian motion (BM) and Ornstein–Uhlenbeck (OU) models^{96,100,101}. We computed 1,000 simulations of single-rate BM and three alternative OU models: BM and OU1 with omnivorous and all carnivorous dietary categories (carnivorous + vermivorous); OU2 with omnivorous, carnivorous, and vermivorous dietary categories; and OU3 with omnivorous, carnivorous, terrestrial vermivorous, and semi-fossorial vermivorous dietary categories. Model fits were compared using differences in the Akaike information criterion (Δ AIC). If earthworm consumption had a deterministic impact on the evolution of one of our measured traits, the best-fitted models should be OU2 or OU3. We ran these analyses with R packages: ape⁸⁹, corpcor¹⁰², mvMORPH¹⁰⁰, phytools⁹¹, and subplex¹⁰³.

To visualize a pattern of convergence in surface area and complexity states, we separately mapped the ratio between olfactory and respiratory turbinal surface area and complexity on the phylogeny. Using maximum likelihood (ML)¹⁰⁴, we estimated ancestral states at internal nodes and interpolated the states along each edge of the phylogeny¹⁰⁵.

To quantify convergence among dietary groups in turbinal surface area, turbinal complexity, snout length, and snout width, we used three measures proposed by Stayton¹⁰⁶. Firstly, C1 is the inverse of the ratio between the phenotypic distance between convergent tips (Dtip) and the maximum distance between any pair of taxa in those two lineages (Dmax). Secondly, C2 is the difference between Dmax and Dtip. Thirdly, C3 is the ratio between C2 and the sum of all phenotypic distances from ancestors to descendants (Ltot.clade). Contrary to C2 and C3, C1 compares phenotypic similarities and phylogenetic relationships without taking into account the absolute amount of evolution that has occurred during convergence¹⁰⁶. We ran these analyses with a modified R package convevol^{107,108}, performing 1,000 simulations.

Data Availability Statement

Raw data are available in the electronic supplementary material (ESM). The CT-scan surfaces could be requested to the corresponding author.

References

- Gould, S. J. & Lewontin, R. C. The spandrels of San Marco and the Panglossian paradigm: a critique of the adaptationist programme. *Proceedings of the Royal Society of London. Series B, Biological sciences* **205**, 581–98 (1979).
- Reeve, H. K. & Sherman, P. W. Adaptation and the Goals of Evolutionary Research. *The Quarterly Review of Biology* **68**, 1–32 (1993).
- McGhee, G. R. *Convergent evolution: limited forms most beautiful*. (MIT Press, 2011).
- Losos, J. B. Convergence, adaptation, and constraint. *Evolution* **65**, 1827–1840 (2011).
- Van Valkenburgh, B., Theodor, J., Friscia, A., Pollack, A. & Rowe, T. Respiratory turbinates of canids and felids: a quantitative comparison. *Journal of Zoology* **264**, 281–293 (2004).
- Brusatte, S. L. *et al.* The Braincase and Neurosensory Anatomy of an Early Jurassic Marine Crocodylomorph: Implications for Crocodylian Sinus Evolution and Sensory Transitions. *The Anatomical Record* **299**, 1511–1530 (2016).
- Pfaff, C., Martin, T. & Ruf, I. Bony labyrinth morphometry indicates locomotor adaptations in the squirrel-related clade (Rodentia, Mammalia). *Proceedings. Biological sciences* **282**, 20150744 (2015).
- Van Valkenburgh, B., Smith, T. D. & Craven, B. A. Tour of a Labyrinth: Exploring the Vertebrate Nose. *The Anatomical Record* **297**, 1975–1984 (2014).
- Van Valkenburgh, B. *et al.* Aquatic adaptations in the nose of carnivorans: evidence from the turbinates. *Journal of Anatomy* **218**, 298–310 (2011).
- Ferreira-Cardoso, S. *et al.* Floccular fossa size is not a reliable proxy of ecology and behaviour in vertebrates. *Scientific Reports* **7**, 2005 (2017).
- Bird, D. J. *et al.* Olfaction written in bone: cribriform plate size parallels olfactory receptor gene repertoires in Mammalia. *Proceedings. Biological sciences* **285**, 20180100 (2018).
- Hayden, S. *et al.* Ecological adaptation determines functional mammalian olfactory subgenomes. *Genome research* **20**, 1–9 (2010).
- Zarzo, M. The sense of smell: molecular basis of odorant recognition. *Biological Reviews* **82**, 455–479 (2007).
- Lindblad-Toh, K. *et al.* Genome sequence, comparative analysis and haplotype structure of the domestic dog. *Nature* **438**, 803–819 (2005).
- Hayden, S. *et al.* A Cluster of Olfactory Receptor Genes Linked to Frugivory in Bats. *Molecular Biology and Evolution* **31**, 917–927 (2014).
- Hughes, G. M. *et al.* The Birth and Death of Olfactory Receptor Gene Families in Mammalian Niche Adaptation. *Molecular Biology and Evolution* **35**, 1390–1406 (2018).
- Negus, V. The Comparative Anatomy and Physiology of the Nose and Paranasal Sinuses Livingstone. *Edinburgh and London* (1958).
- Laska, M., Genzel, D. & Wieser, A. The Number of Functional Olfactory Receptor Genes and the Relative Size of Olfactory Brain Structures Are Poor Predictors of Olfactory Discrimination Performance with Enantiomers. *Chemical Senses* **30**, 171–175 (2005).
- Frasnelli, J. *et al.* Neuroanatomical correlates of olfactory performance. *Experimental Brain Research* **201**, 1–11 (2010).
- Seubert, J., Freiherr, J., Frasnelli, J., Hummel, T. & Lundstrom, J. N. Orbitofrontal Cortex and Olfactory Bulb Volume Predict Distinct Aspects of Olfactory Performance in Healthy Subjects. *Cerebral Cortex* **23**, 2448–2456 (2013).
- Smith, T. D., Eiting, T. P. & Rossie, J. B. Distribution of Olfactory and Nonolfactory Surface Area in the Nasal Fossa of *Microcebus murinus*: Implications for Microcomputed Tomography and Airflow Studies. *The Anatomical Record: Advances in Integrative Anatomy and Evolutionary Biology* **294**, 1217–1225 (2011).
- Rowe, T. B., Eiting, T. P., Macrini, T. E. & Ketcham, R. A. Organization of the Olfactory and Respiratory Skeleton in the Nose of the Gray Short-Tailed Opossum *Monodelphis domestica*. *Journal of Mammalian Evolution* **12**, 303–336 (2005).
- Green, P. A. *et al.* Respiratory and olfactory turbinal size in canid and arctoid carnivorans. *Journal of Anatomy* **221**, 609–621 (2012).
- Barrios, A. W., Núñez, G., Quinteiro, P. S., Salazar, I. & Chameró, P. Anatomy, histochemistry, and immunohistochemistry of the olfactory subsystems in mice. <https://doi.org/10.3389/fnana.2014.00063> (2014).
- Ruben, J. A. *et al.* The Metabolic Status of Some Late Cretaceous Dinosaurs. *Science* **273**, 1204–1207 (1996).
- Schmidt-Nielsen, K., Hainsworth, F. R. & Murrish, D. E. Counter-current heat exchange in the respiratory passages: Effect on water and heat balance. *Respiration Physiology* **9**, 263–276 (1970).
- Hillenius, W. J. The evolution of nasal turbinates and mammalian endothermy. *Paleobiology* **18**, 17–29 (1992).
- Craven, B. A. *et al.* Reconstruction and Morphometric Analysis of the Nasal Airway of the Dog (*Canis familiaris*) and Implications Regarding Olfactory Airflow. *The Anatomical Record: Advances in Integrative Anatomy and Evolutionary Biology* **290**, 1325–1340 (2007).
- Craven, B. A., Paterson, E. G. & Settles, G. S. The fluid dynamics of canine olfaction: unique nasal airflow patterns as an explanation of macrosmia. *Journal of the Royal Society, Interface* **7**, 933–43 (2010).
- Morgan, K. T., Kimbell, J. S., Monticello, T. M., Patra, A. L. & Fleishman, A. Studies of inspiratory airflow patterns in the nasal passages of the F344 rat and rhesus monkey using nasal molds: Relevance to formaldehyde toxicity. *Toxicology and Applied Pharmacology* **110**, 223–240 (1991).
- Kimbell, J. S. *et al.* Computer Simulation of Inspiratory Airflow in All Regions of the F344 Rat Nasal Passages. *Toxicology and Applied Pharmacology* **145**, 388–398 (1997).
- Lester, C. W. & Costa, D. P. Water conservation in fasting northern elephant seals (*Mirounga angustirostris*). *The Journal of experimental biology* **209**, 4283–94 (2006).
- Eiting, T. P., Smith, T. D., Perot, J. B. & Dumont, E. R. The role of the olfactory recess in olfactory airflow. *The Journal of experimental biology* **217**, 1799–803 (2014).
- Allison, A. C. The morphology of the olfactory system in the vertebrates. *Biological Reviews* **28**, 195–244 (1953).
- Ressler, K. J., Sullivan, S. L. & Buck, L. B. A zonal organization of odorant receptor gene expression in the olfactory epithelium. *Cell* **73**, 597–609 (1993).
- Van Valkenburgh, B. *et al.* Respiratory and Olfactory Turbinates in Feliform and Caniform Carnivorans: The Influence of Snout Length. *The Anatomical Record* **297**, 2065–2079 (2014).
- Firestein, S. How the olfactory system makes sense of scents. *Nature* **413**, 211–218 (2001).
- Ruf, I. Comparative Anatomy and Systematic Implications of the Turbinal Skeleton in Lagomorpha (Mammalia). *The Anatomical Record* **297**, 2031–2046 (2014).
- Maier, W. & Ruf, I. Morphology of the Nasal Capsule of Primates-With Special Reference to *Daubentonia* and *Homo*. *The Anatomical Record* **297**, 1985–2006 (2014).
- Reinbach, W. Zur Entwicklung des Primordialcraniums von *Dasybus novemcinctus* Linné (*Tatusia novemcincta* Lesson) I. *Zeitschrift für Morphologie und Anthropologie* 375–444. <https://doi.org/10.2307/25753216> (1952).
- Reinbach, W. Zur Entwicklung des Primordialcraniums von *Dasybus novemcinctus* Linné (*Tatusia novemcincta* Lesson) II. *Zeitschrift für Morphologie und Anthropologie* 1–72. <https://doi.org/10.2307/25753226> (1952).
- Yee, K. K., Craven, B. A., Wysocki, C. J. & Van Valkenburgh, B. Comparative Morphology and Histology of the Nasal Fossa in Four Mammals: Gray Squirrel, Bobcat, Coyote, and White-Tailed Deer. *The Anatomical Record* **299**, 840–852 (2016).
- Fabre, P.-H. *et al.* A new genus of rodent from Wallacea (Rodentia: Muridae: Murinae: Rattini), and its implication for biogeography and Indo-Pacific Rattini systematics. *Zoological Journal of the Linnean Society* **169**, 408–447 (2013).

44. Rowe, K. C., Achmadi, A. S. & Esselstyn, J. A. Repeated evolution of carnivory among Indo-Australian rodents. *Evolution* **70**, 653–665 (2016).
45. Musser, G. G. & Durden, L. A. Morphological and Geographic Definitions of the Sulawesi Shrew Rats *Echiothrix leucura* and *E. centrosa* (Muridae, Murinae), and Description of a New Species of Sucking Louse (Phthiraptera: Anoplura). *Bulletin of the American Museum of Natural History* **391**, 1–87 (2014).
46. Balete, D. S. *et al.* Archboldomys (Muridae: Murinae) Reconsidered: A New Genus and Three New Species of Shrew Mice from Luzon Island, Philippines. *American Museum Novitates* **3754**, 1–60 (2012).
47. Esselstyn, J. A., Achmadi, A. S. & Rowe, K. C. Evolutionary novelty in a rat with no molars. *Biology letters* **8**, 990–3 (2012).
48. Samuels, J. Cranial morphology and dietary habits of rodents. *Zoological Journal of the Linnean Society* **156**, 864–888 (2009).
49. Lebrun, R. MorphoDig, an open-source 3d freeware dedicated to biology. available at <http://morphomuseum.com/morphodig> (2018).
50. Heth, G. & Todrank, J. In *Subterranean Rodents* 85–96, https://doi.org/10.1007/978-3-540-69276-8_8 (Springer Berlin Heidelberg, 2007).
51. Musser, G. G. Crunomys and the small-bodied shrew rats native to the Philippine Islands and Sulawesi (Celebes). *Bulletin of the AMNH* **174**, (1982).
52. Heaney, L. R., Balete, D. S. & Rickart, E. A. *The mammals of Luzon Island: biogeography and natural history of a Philippine fauna*. (Johns Hopkins University Press, Baltimore, 2016).
53. McIntosh, A. F. & Cox, P. G. The impact of digging on craniodental morphology and integration. *Journal of Evolutionary Biology* **29**, 2383–2394 (2016).
54. Gomes Rodrigues, H., Šumbera, R. & Hautier, L. Life in Burrows Channelled the Morphological Evolution of the Skull in Rodents: the Case of African Mole-Rats (Bathyergidae, Rodentia). *Journal of Mammalian Evolution* **23**, 175–189 (2016).
55. Rickart, E. A., Heaney, L. R. & Uzzurum, R. C. B. Distribution and Ecology of Small Mammals along an Elevational Transect in Southeastern Luzon, Philippines. *Journal of Mammalogy* **72**, 458–469 (1991).
56. Heaney, L. R., Balete, D. S., Rosell-Ambal, R. G. B., Veluz, M. J. & Rickart, E. A. The Small Mammals of Mt. Banahaw - San cristobal national Park, Luzon, Philippines: elevational distribution and ecology of a highly endemic Fauna. *National Museum of the Philippines: Journal of Natural History* **1**, 49–64 (2013).
57. Rickart, E. A., Heaney, L. R., Balete, D. S. & Tabaranza, B. R. Small mammal diversity along an elevational gradient in northern Luzon, Philippines. *Mammalian Biology - Zeitschrift für Säugetierkunde* **76**, 12–21 (2011).
58. McGann, J. P. Poor human olfaction is a 19th-century myth. *Science (New York, N.Y.)* **356**, eaam7263 (2017).
59. Laska, M. & Seibt, A. Olfactory sensitivity for aliphatic alcohols in squirrel monkeys and pigtail macaques. *Journal of Experimental Biology* **205**, (2002).
60. Musser, G. G. Sulawesi Rodents: Species Traits and Chromosomes of *Haeromys minahassae* and *Echiothrix leucura* (Muridae: Murinae). *American Museum Novitates* **2989**, 1–18 (1990).
61. Musser, G. G. & Lunde, D. P. Systematic Reviews of New Guinea *Coccymys* and 'Melomys' *Albidens* (Muridae, Murinae) with Descriptions of New Taxa. *Bulletin of the American Museum of Natural History* **329**, 1–139 (2009).
62. Charles, C., Solé, F., Rodrigues, H. G. & Viriot, L. Under pressure? Dental adaptations to termitophagy and vermivory among mammals. *Evolution* **67**, 1792–1804 (2013).
63. Jackson, D. C. & Schmidt-Nielsen, K. Countercurrent heat exchange in the respiratory passages. *Proceedings of the National Academy of Sciences of the United States of America* **51**, 1192–7 (1964).
64. Rowe, K. C., Achmadi, A. S. & Esselstyn, J. A. A new genus and species of omnivorous rodent (Muridae: Murinae) from Sulawesi, nested within a clade of endemic carnivores. *Journal of Mammalogy* **97**, 978–991 (2016).
65. Muschick, M., Indermaur, A. & Salzburger, W. Convergent Evolution within an Adaptive Radiation of Cichlid Fishes. *Current Biology* **22**, 2362–2368 (2012).
66. Losos, J. B. & Ricklefs, R. E. Adaptation and diversification on islands. *Nature* **457**, 830–836 (2009).
67. Esselstyn, J. A., Achmadi, A. S., Handika, H. & Rowe, K. C. A hog-nosed shrew rat (Rodentia: Muridae) from Sulawesi Island, Indonesia. *Journal of Mammalogy* **96**, 895–907 (2015).
68. Musser, G. G. Crunomys and the small-bodied shrew rats native to the Philippine Islands and Sulawesi (Celebes). Bulletin of the AMNH; v. 174, article 1. (1982).
69. Musser, G. G. Results of the Archbold Expeditions. No. 91 A New Genus and Species of Murid Rodent from Celebes, with a Discussion of its Relationships. *American Museum Novitates* (1969).
70. Collins, N. M. The Distribution of Soil Macrofauna on the West Ridge of Gunung (Mount) Mulu, Sarawak. *Oecologia* **44**, 263–275 (1980).
71. Samson, D. A., Rickart, E. A. & Gonzales, P. C. Ant Diversity and Abundance along an Elevational Gradient in the Philippines. *Biotropica* **29**, 349–363 (1997).
72. Heaney, L. R. Small mammal diversity along elevational gradients in the Philippines: an assessment of patterns and hypotheses. *Global Ecology and Biogeography* **10**, 15–39 (2001).
73. Heaney, L. R. Mammalian species richness on islands on the Sunda Shelf, Southeast Asia. *Oecologia (Berlin)* **61**, 11–17 (1984).
74. Nor, S. M. Elevational diversity patterns of small mammals on Mount Kinabalu, Sabah, Malaysia. *Global Ecology and Biogeography* **10**, 41–62 (2001).
75. Balete, D. S., Heaney, L. R., Josefa Veluz, M. & Rickart, E. A. Diversity patterns of small mammals in the Zambales Mts., Luzon, Philippines. *Mammalian Biology - Zeitschrift für Säugetierkunde* **74**, 456–466 (2009).
76. Yohe, L. R., Hoffmann, S. & Curtis, A. Vomeronasal and Olfactory Structures in Bats Revealed by DiceCT Clarify Genetic Evidence of Function. *Frontiers in neuroanatomy* **12**, 32 (2018).
77. Wagner, F. & Ruf, I. Who nose the borzoi? Turbinal skeleton in a dolichocephalic dog breed (*Canis lupus familiaris*). *Mammalian Biology*, <https://doi.org/10.1016/J.MAMBIO.2018.06.005> (2018).
78. Schreider, J. P. & Raabe, O. G. Anatomy of the nasal-pharyngeal airway of experimental animals. *The Anatomical Record* **200**, 195–205 (1981).
79. Rygg, A. D., Van Valkenburgh, B. & Craven, B. A. The Influence of Sniffing on Airflow and Odorant Deposition in the Canine Nasal Cavity. *Chemical Senses* **42**, 683–698 (2017).
80. Ruf, I. Vergleichend-ontogenetische Untersuchungen an der Ethmoidalregion der Muroidea (Rodentia, Mammalia). Ein Beitrag zur Morphologie und Systematik der Nagetiere. (2004).
81. Macrini, T. E. Comparative Morphology of the Internal Nasal Skeleton of Adult Marsupials Based on X-ray Computed Tomography. *Bulletin of the American Museum of Natural History* **365**, 1–91 (2012).
82. Smith, T. D., Rossie, J. B. & Bhatnagar, K. P. Evolution of the nose and nasal skeleton in primates. *Evolutionary Anthropology: Issues, News, and Reviews* **16**, 132–146 (2007).
83. Musser, G. G. A Systematic Review of Sulawesi *Bunomys* (Muridae, Murinae) with the Description of Two New Species. *Bulletin of the American Museum of Natural History* **392**, 1–313 (2014).
84. Smith, T. G., Lange, G. D. & Marks, W. B. Fractal methods and results in cellular morphology—dimensions, lacunarity and multifractals. *Journal of neuroscience methods* **69**, 123–36 (1996).
85. Karperien, A. L., Jelinek, H. F., Buchan, A. M. & Karperien, A. Box-counting analysis of microglia form in schizophrenia, Alzheimer's disease and affective disorder. *Fractals* **16**, 103–107 (2008).

86. Rasband, W. S. ImageJ: Image processing and analysis in Java. *Astrophysics Source Code Library, record ascl:1206.013* (2012).
87. Karpertien, A. User's guide for FraCLac for ImageJ, version 2.5. (2012).
88. Team R-Core. R: A language and environment for statistical computing. *R Foundation for Statistical Computing, Vienna, Austria*. (2017).
89. Paradis, E., Claude, J. & Strimmer, K. APE: Analyses of Phylogenetics and Evolution in R language. *Bioinformatics* **20**, 289–290 (2004).
90. Pinheiro, J., Bates, D., DebRoy, S., Sarkar, D. & Team, R. C. nlme: linear and nonlinear mixed effects models. *R package version 3*, 1–117 (2014).
91. Revell, L. J. phytools: an R package for phylogenetic comparative biology (and other things). *Methods in Ecology and Evolution* **3**, 217–223 (2012).
92. Steppan, S. J. & Schenck, J. J. Muroid rodent phylogenetics: 900-species tree reveals increasing diversification rates. *PLOS ONE* **12**, e0183070 (2017).
93. Claude, J. *Morphometrics with R*. (Springer, 2008).
94. Hothorn, T. *et al.* Package 'multcomp'. (2017).
95. Grafen, A. The phylogenetic regression. *Philosophical transactions of the Royal Society of London. Series B, Biological sciences* **326**, 119–57 (1989).
96. Butler, M. A. & King, A. A. Phylogenetic Comparative Analysis: A Modeling Approach for Adaptive Evolution. *The American Naturalist* **164**, 683–695 (2004).
97. García-Berthou, E. On the misuse of residuals in ecology: testing regression residuals vs. the analysis of covariance. *Journal of Animal Ecology* **70**, 708–711 (2001).
98. Freckleton, R. P. The seven deadly sins of comparative analysis. *Journal of Evolutionary Biology* **22**, 1367–1375 (2009).
99. Freckleton, R. P. On the misuse of residuals in ecology: regression of residuals vs. multiple regression. *Journal of Animal Ecology* **71**, 542–545 (2002).
100. Clavel, J., Escarguel, G. & Merceron, G. mv morph: an r package for fitting multivariate evolutionary models to morphometric data. *Methods in Ecology and Evolution* **6**, 1311–1319 (2015).
101. Hansen, T. F. Stabilizing Selection and the Comparative Analysis of Adaptation. *Evolution* **51**, 1341 (1997).
102. Schaefer, J. *et al.* corpcor: Efficient estimation of covariance and (partial) correlation. *R package version 1*, (2013).
103. King, A. & King, M. Package 'subplex'. (2016).
104. Felsenstein, J. Phylogenies and the Comparative Method. *The American Naturalist* **125**, 1–15 (1985).
105. Revell, L. J. Two new graphical methods for mapping trait evolution on phylogenies. *Methods in Ecology and Evolution* **4**, 754–759 (2013).
106. Stayton, C. T. The definition, recognition, and interpretation of convergent evolution, and two new measures for quantifying and assessing the significance of convergence. *Evolution* **69**, 2140–2153 (2015).
107. Stayton, A. C. T. & Stayton, M. C. T. Package 'convevol': Analysis of Convergent Evolution. (2017).
108. Zelditch, M. L., Ye, J., Mitchell, J. S. & Swiderski, D. L. Rare ecomorphological convergence on a complex adaptive landscape: Body size and diet mediate evolution of jaw shape in squirrels (Sciuridae). *Evolution* **71**, 633–649 (2017).

Acknowledgements

We thank: S. Cardoso, M. Wright, J. Clavel, I. Ruf, R. Allio, J. Claude, L. Hautier, C. Molinier, F. Delsuc, M. Orliac, and G.G. Musser. 3D data acquisitions were performed using the μ -CT facilities of the MRI platform member of the national infrastructure France-BioImaging supported by the French National Research Agency (ANR-10-INBS-04, «Investments for the future»), and of the Labex CEMEB (ANR-10-LABX-0004) and NUMEV (ANR-10-LABX-0020). Thanks to F. Ahmed, B. Clark, and V. Fernandez for access to the CT-scan facilities at the Natural History Museum (NHMUK, London). We are grateful to the following people and institutions for granting access to specimens: S. Morand with ANR 07 BDIV 012 CERoPath, S. Ginot, J. Claude, F. Veyrunes, F. Bonhomme, and J. J. Duquesne (UM2); Y. Chaval and N. Charbonnel (CBGP); P. Jenkins, S. Oxford, and K. Dixey (NHMUK, London); D. Wilson, L. Gordon, and D. Lunde (USNM, Washington, D.C.); E. Westwig, M. Surovy, N. Duncan, C. Grohé, and R. S. Voss (AMNH, New York); K. Roberts and K. M.C. Rowe (NMV, Melbourne); D. S. Balet, A. Ferguson, and W. T. Stanley (FMNH, Chicago); G. Véron, V. Nicolas, and C. Denys (MNHN, Paris); S. van Der Mije (RMNH, Leiden). Likewise, we thank the Research Center for Biology, Indonesian Institute of Sciences (RCB-LIPI) and the Museum Zoologicum Bogoriense for providing staff, and support to carry out fieldwork in the Wallacea. This research received support from: SYNTHESYS Project which is financed by the European Community Research Infrastructure Action (FP7: GB-TAF-5737, GB-TAF-6945 to the NHM UK), Agence Nationale de la Recherche (Défi des autres savoirs, DS10, ANR-17-CE02-0005 RHINOGRAD 2017), PEPS ADAPTATION ADAPTABILITE (SHREWNose), Negaunee Foundation, Field Museum's Barbara Brown Fund for Mammal Research National Science Foundation (DEB-1441634, DEB-1343517, OISE-0965856), and National Geographic Society (9025-11). This is contribution of ISEM SUD N°2018-243, Univ Montpellier, CNRS, EPHE, IRD, Montpellier, France.

Author Contributions

Q.M. and P.H.F. designed the study, collected most of CT-scan data, performed analyses, and drafted the first manuscript. A.S.A., K.C.R., L.R.H. and J.A.E. collected most Sulawesi and Philippines specimens. A.R.E. made available half of Sulawesi CT-scan data. R.L. designed the 3D complexity method and implemented it in the freeware MorphoDig. A.R.E., A.S.A., K.C.R., L. R. H., J.A.E., R.L. and R.P.M. significantly and critically improved the manuscript. Authors gave final approval for publication.

Additional Information

Supplementary information accompanies this paper at <https://doi.org/10.1038/s41598-018-35827-0>.

Competing Interests: The authors declare no competing interests.

Publisher's note: Springer Nature remains neutral with regard to jurisdictional claims in published maps and institutional affiliations.



Open Access This article is licensed under a Creative Commons Attribution 4.0 International License, which permits use, sharing, adaptation, distribution and reproduction in any medium or format, as long as you give appropriate credit to the original author(s) and the source, provide a link to the Creative Commons license, and indicate if changes were made. The images or other third party material in this article are included in the article's Creative Commons license, unless indicated otherwise in a credit line to the material. If material is not included in the article's Creative Commons license and your intended use is not permitted by statutory regulation or exceeds the permitted use, you will need to obtain permission directly from the copyright holder. To view a copy of this license, visit <http://creativecommons.org/licenses/by/4.0/>.

© The Author(s) 2018